9-2004

A simple design for an electronic speckle pattern interferometer

Thomas R. Moore
Department of Physics, Rollins College, TMOORE@rollins.edu

Published In
Thomas R. Moore, "A simple design for an electronic speckle pattern interferometer," American Journal of Physics 72, 1380-1384 (2004). With erratum, American Journal of Physics 73, 189 (2005).

A simple design for an electronic speckle pattern interferometer

Thomas R. Moore[a)]
Department of Physics, Rollins College, 1000 Holt Avenue, Winter Park, Florida 32789

(Received 6 April 2004; accepted 10 June 2004)

An electronic speckle pattern interferometer suitable for use in an undergraduate laboratory is described. This interferometer can be built for a small fraction of the cost of a commercial version and is simple and inexpensive to build and understand. The interferometer is useful for visualizing the normal modes of vibrating objects as well as changes in index of refraction.

[DOI: 10.1119/1.1778396]

I. INTRODUCTION

The electronic speckle pattern interferometer is a valuable tool for studying the vibrations of objects, as well as visualizing changes in the index of refraction. The results are very similar to those obtained using holographic interferometry, and the process is sometimes inaccurately referred to as TV holography. The electronic speckle pattern interferometer has been well studied in the recent past, and is a useful tool for researchers in many fields. An excellent review of holographic and speckle interferometry can be found in Ref. 1.

Because of the ease with which the vibrations and small displacements of objects can be studied in real time, the electronic speckle pattern interferometer is the ideal tool for the undergraduate laboratory as well as for classroom demonstrations. The patterns of normal modes of vibration are especially dramatic when viewed using an electronic speckle pattern interferometer, and it is the ideal method for demonstrating unusual phenomena such as the splitting of the degenerate normal modes of vibration due to asymmetries.[2] Unfortunately, a commercial electronic speckle pattern interferometer costs well over $50,000. Such an expense is difficult to justify for a demonstration apparatus even if funds of that magnitude are available.

An alternative to buying an electronic speckle pattern interferometer is to build one from discrete optical components. There are several of these in use, but the cost and difficulty of building one is often daunting. We present a design for an electronic speckle pattern interferometer that can be built using items commonly found in an undergraduate optics laboratory. This electronic speckle pattern interferometer enables students to visually detect the normal modes of vibrating structures, visualize atmospheric aberrations caused by heat flow or convection, and measure submicron displacements. The design is simple enough that constructing the interferometer is an ideal project for an undergraduate student.

We begin by introducing the electronic speckle pattern interferometer. We outline the theory and discuss the issues surrounding building one. We then describe a new design that eliminates the most difficult part of constructing an interferometer of this type. We conclude with a discussion of some typical results and an example of how the interferometer can be useful in the context of a classroom or undergraduate research laboratory.

II. THE ELECTRONIC SPECKLE PATTERN INTERFEROMETER

An electronic speckle pattern interferometer relies on the correlation between two speckle patterns, each one created by the interference between a reference beam and the image of an object illuminated by a laser. Typically the two images are of an object before and after some deformation. Although there are several variations on the basic design, the interferometer of interest here uses image subtraction to correlate the two images. The process of measuring the correlation between the two images does not need to be accomplished electronically and was originally accomplished using film; however, the electronic subtraction process makes the interferogram easy to form, view, and record in real time.

Here we are concerned primarily with observing and measuring out of plane displacements of periodically moving objects such as vibrating plates. A simplified diagram of the version of the electronic speckle pattern interferometer most often used for this purpose is shown in Fig. 1. Light from a laser is separated into two beams; one beam serves to illuminate the object under study and the other acts as a reference beam. The object is imaged onto a charge coupled device (CCD) array through a beamsplitter, which serves to insert the reference beam into the optical path. The image forming optics and the optics for the reference beam are designed so that the two beams appear to emerge from the exit pupil of the imaging lens system and therefore have the same divergence. The combined beams form an image on a CCD array or some other video capture device.

To view the effects of movement of the object, an image is stored before the object is displaced. A second image is obtained after displacement and the two images are subtracted. The absolute values of the subtracted pixel values are then multiplied by a constant and displayed on a computer monitor. Pixels where the speckle pattern has not changed between the two images will subtract to zero and be displayed as black. Pixels in positions where the speckle pattern has changed will have a nonzero value and will be displayed as a shade of gray or white.

A. Theory

A detailed theory of the operation of the electronic speckle pattern interferometer can be found in Refs. 1 and 3, but for the purposes of this article a heuristic understanding will suffice.

We begin our discussion by assuming the simplified arrangement shown in Fig. 2. We assume that the illuminating beam is incident on the object at near normal incidence, and

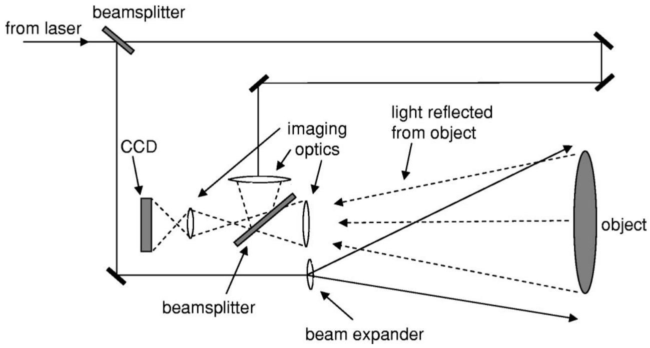

Fig. 1. Schematic of an electronic speckle pattern interferometer that is sensitive to out of plane displacement.

the image is coincident on an image plane with the coherent reference beam. The object plane is designated by a coordinate system with primes and the image plane is in the unprimed coordinate system. If we designate the irradiance of the image beam at the image plane as I_i and the irradiance of the reference beam as I_r, then the irradiance of the composite image on the array is given by

$$I_0(\mathbf{r}) = I_i + I_r + 2\sqrt{I_i I_r}\cos[\epsilon(\mathbf{r})]. \tag{1}$$

The irradiance of both beams is assumed to be uniform across the field, and the phase of the reference beam is assumed to be equal to the mean phase of the image beam across the field because they both appear to emanate from the exit pupil. The phase angle $\epsilon(\mathbf{r})$ is a function of position due to the nonuniform phase of the image bearing beam caused by the roughness of the surface of the object.

When a point on the object is displaced a distance $\delta z'$, the phase change in the image plane is given by

$$\Delta\epsilon(\mathbf{r}) = \frac{4\pi\delta z'(\mathbf{r}')}{\lambda}, \tag{2}$$

where λ is the wavelength of the light and $\mathbf{r}$ is conjugate to $\mathbf{r}'$. After displacement, the irradiance on the array is given by

$$I_1(\mathbf{r}) = I_i + I_r + 2\sqrt{I_i I_r}\cos[\epsilon(\mathbf{r}) + \Delta\epsilon(\mathbf{r})]. \tag{3}$$

Clearly the maximum correlation between Eqs. (1) and (3) will occur when $\Delta\epsilon(\mathbf{r}) = 2n\pi$, where n is an integer, and the minimum correlation will occur when $\Delta\epsilon(\mathbf{r}) = (2n+1)\pi$. A formal proof can be found in Appendix E of Ref. 1. When

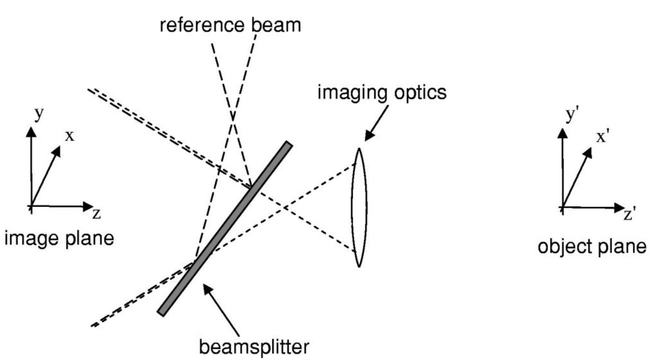

Fig. 2. Simplified schematic of the optical system of an electronic speckle pattern interferometer. Coordinates in the object plane are designated by primes; the image plane is in the unprimed coordinate system.

the two images are subtracted, regions of complete correlation will sum to zero while decorrelated regions will not. The value of the subtraction of the two decorrelated images, and hence, the image contrast, will depend primarily on the speckle size, with the maximum contrast achieved when the speckle size is equal to the size of the pixels. The mean diameter of the speckle size can be estimated for this situation by[4]

$$d \approx 1.22(1+M)\lambda F, \tag{4}$$

where M is the magnification of the image and F is the aperture ratio of the lens (the f number). The result of the subtraction process will be an image of the object with dark fringes where the displacement of the object results in a phase change of even multiples of π and bright fringes in places where the phase change is an odd multiple of π.

It is obvious from this discussion that electronic speckle pattern interferometry is very effective at visualizing and measuring small out of plane displacements; however, it also is commonly used to visualize the harmonic vibrations of objects. Typically these observations are accomplished using time-averaged electronic speckle pattern interferometry.

In its simplest manifestation, time-averaged electronic speckle pattern interferometry is accomplished by vibrating the object under study at a single frequency and subtracting the image of the vibrating structure from the original stored image taken before the onset of vibration. In this case Eq. (2) becomes

$$\Delta\epsilon(\mathbf{r},\omega) = \frac{4\pi\delta z'(\mathbf{r}')}{\lambda}\cos\omega t, \tag{5}$$

where ω is the angular frequency of the vibration. When the integration time of the detector significantly exceeds the period of vibration, the effect is to average the phase difference and the result is given by[1]

$$I_\omega(\mathbf{r}) = I_i + I_r + 2\sqrt{I_i I_r}\cos(\epsilon(\mathbf{r}))J_0\left(\frac{4\pi}{\lambda}\delta z'(\mathbf{r}')\right), \tag{6}$$

where J_0 represents the zero-order Bessel function of the first kind. The intensity of the image viewed on the display is found by subtracting Eq. (6) from Eq. (1) and taking the absolute value of the result. Thus, to within a constant the intensity of the final image is given by

$$I(\mathbf{r}) = 1 - J_0\left(\frac{4\pi}{\lambda}\delta z'(\mathbf{r}')\right). \tag{7}$$

Inspection of Eq. (7) reveals that the minima in the intensity will occur at the maxima of J_0, which are unevenly spaced but easily calculated or found in tables. A reasonable estimate of the spacing is that the first few maxima are separated by integer multiples of $\delta z'(\mathbf{r}') \sim \lambda/2$. [The actual values for $\delta z'(\mathbf{r}')$ for the first two maxima are 0.56λ and 1.06λ.]

Note that the fringe visibility is limited by the value of J_0, which is unity for $\delta z'(\mathbf{r}') = 0$, but has a value of only ~ 0.3 at the first maximum and decreases rapidly for subsequent maxima; therefore, the fringe visibility will be significantly less than unity. Additionally, the speckle appearance remains in the final image, further degrading the fidelity of the result. Methods for improving fringe contrast are discussed in Refs. 5 and 6 and the visibility of the speckle can be reduced by appropriate spatial filtering of the image. However, in the undergraduate laboratory and for many research applications,

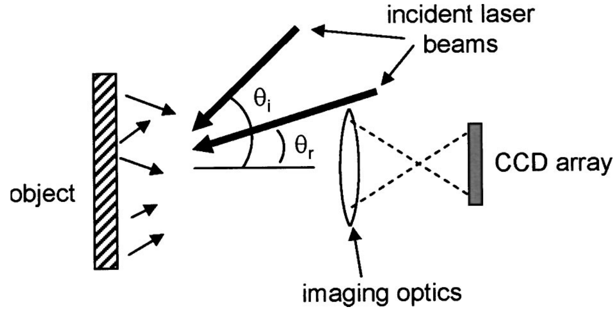

Fig. 3. An electronic speckle pattern interferometer using a simplified optical arrangement. Although this arrangement eliminates the need for a complex optical system, it results in reduced sensitivity to out of plane displacement.

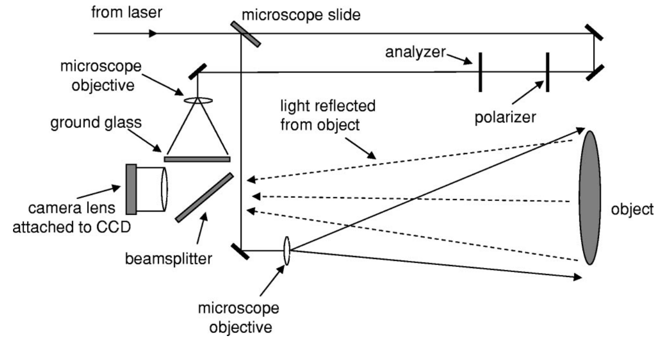

Fig. 4. Schematic of an electronic speckle pattern interferometer that does not require a complicated optical arrangement but does not have reduced sensitivity.

the fringe visibility is more than adequate without resorting to methods that increase the complexity of the apparatus. In cases where the image contrast is not sufficient for publication, postprocessing of the final image with commercially available software is usually sufficient.

B. Construction of an interferometer

An interferometer such as we have described and shown in Fig. 1 consists largely of commonly available components. The single exception is the optics required to combine the image and reference beam. This arrangement requires the design of a specific lens system for both the imaging lens and the reference beam. Given the outstanding quality of inexpensive commercially available camera lenses, we wish to image the object using one of these lenses. However, to do so requires some careful optical engineering because a beamsplitter must be inserted between the lens and the detector and the spacing must be such that the curvature of the reference beam makes it appear to the detector as if it originates at the exit pupil of the imaging optical system. Engineering an optical system that meets these stringent requirements requires some skill and expense and inevitably reduces the fidelity of the imaging system.

Although these requirements are not insurmountable, the necessary optical engineering to design such a system and the expense of doing it might be daunting. One way to eliminate the need for this cumbersome arrangement is to have the reference beam and the image beam illuminate the surface of the object as shown in Fig. 3. In this arrangement the need for combining the reference beam and the object beam prior to them reaching the detector is eliminated at the cost of reduced sensitivity. In this case the phase factor in Eq. (3) becomes

$$\Delta\epsilon(\mathbf{r}) = \frac{2\pi\delta z'(\mathbf{r}')}{\lambda}(\cos\theta_r - \cos\theta_i), \tag{8}$$

where θ_i and θ_r are the angles of incidence of the image and reference beams as shown in Fig. 3. (The terms image beam and reference beam lose their meaning in this arrangement.)

Efforts have been made to maintain the maximum sensitivity as well eliminate the need for a complex optical systems;[7,8] however, these designs require specially manufactured beamsplitters with a series of transparent, opaque, and mirror stripes. This arrangement decreases the complexity of the optical system, but the beamsplitters must be custom made and perfectly aligned.

We have designed an electronic speckle pattern interferometer that is simple to construct but does not sacrifice sensitivity for simplicity. The design is shown in Fig. 4. In this design the optical system used for imaging in the design shown in Fig. 1 is replaced by a beamsplitter and a plate of ground glass placed before the imaging optics. In this way a commercial camera lens can be attached to a commercial CCD array in the usual manner. The smooth reference beam is now replaced by a speckled reference beam, but the mean speckle size on the imaging array is not affected because it depends only on the imaging optics and not on the details of the object being illuminated.[4] The analysis of the system is unchanged from that presented previously with the exception that the irradiance of the reference beam contains a position dependent phase. Therefore, Eqs. (3) and (6) describe the output of this interferometer as well as the more familiar version shown in Fig. 1.

To minimize the cost, it should not be necessary for the source to have a high output power. Because a typical HeNe laser may produce only a few milliwatts of power, the object under study or the f number of the imaging lens must be small. A small f-number lens results in a speckle size at the image plane that is smaller than a typical pixel; however, as we show in the following, the speckle size can be significantly smaller than the pixel size before the system becomes unusable.

III. RESULTS

Here we describe the performance of a system built as shown in Fig. 4. The design is optimized for low cost, but commonly available optical hardware can improve the ease and quality of the image if it is available. For example, the apparatus shown in Fig. 4 uses a microscope slide acting as a beam splitter and polarizers to provide variability in the intensity of the reference beam. This arrangement can be replaced by a polarizing beam splitter bracketed by a half wave plate on either side, which will allow for easier balancing of the intensities of the reference and image beams. However, cost is often a significant factor, so we have constructed the apparatus as shown to demonstrate that it is quite adequate for many applications.

The light source used was a 15 mW HeNe laser ($\lambda = 632$ nm). This laser provided sufficient power to illuminate an area approximate 50 cm in diameter. A 2-mm-thick circular metal plate ≈ 17 cm in diameter and painted flat white was used as the object of study. The imaging beam was

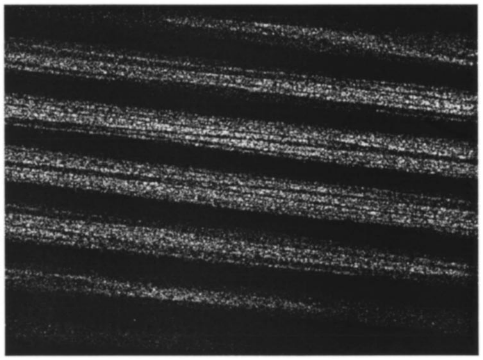

Fig. 5. Interferograms of a 17 cm circular plate vibrating in one of its normal modes. Theoretically the two modes occur at the same frequency, however, the degeneracy is broken by a slight asymmetry in the plate. The frequencies of vibration are 2133 and 2145 Hz.

expanded using a microscope objective and then directed toward the metal plate. The reference beam was directed around a delay leg and expanded through a microscope objective before illuminating a piece of ground glass. A 2 in. square 50/50 beamsplitter was oriented at 45° to the direction of observation and placed directly in front of the imaging lens. The imaging system consisted of a commercially available $f/1.2$ C-mount camera lens mounted to a standard CCD camera with a 6.4×4.8 mm sensing area and 8.4×9.8 μm pixel size.

Real time image processing was accomplished using a desktop computer and a LabView program written by the author. The software subtracted the real-time image from the reference image and multiplied each pixel value by a factor of 20. Of the components needed for the construction of the interferometer, the computer interface and the software package for image subtraction were the most expensive components not commonly found in undergraduate laboratories. It is possible to use less sophisticated hardware and software, and image subtraction can even be accomplished after the fact using freely available imaging software. However, the ability to view the image in real time is very valuable from an educational standpoint, and we recommend some form of real-time image subtraction.

If we substitute the values for the wavelength and f number into Eq. (4), we find that the mean speckle size is approximately ten times smaller than the pixel size. Whenever the speckle size is smaller than the pixel size, there is a significantly reduced fringe visibility, and various methods have been devised to overcome this problem.[5,6] The stability of the platform on which the interferometer is built is also an issue because vibrations will tend to decorrelate the speckle. The easiest and most efficient method of mitigating the effects of external vibrations is to mount the entire apparatus on a vibration isolated optical table, but other methods also have been investigated.[9]

Although all phenomena that can decorrelate the speckle should be minimized to maximize the efficiency of the system, for many applications the reduction in sensitivity due to ambient vibrations and reduced fringe contrast is not severe enough to be of concern. For example, Fig. 5 contains images of the circular plate vibrating in one of its normal modes. These images were made using the system described previously with all of the components mounted on a small optical table with no vibration isolation. The vibrations of the plate were driven acoustically by connecting a function generator to an amplifier and placing the speaker near the plate. Although the image contrast can be improved with postprocessing, the images shown in Fig. 5 were taken directly from the real-time image with no enhancement. Clearly the image quality is sufficient for instructional purposes as well as for many research purposes.

The images shown in Fig. 5 are an excellent example of the usefulness of this type of interferometer for instructional purposes. When discussing normal modes of vibration, it is common to demonstrate one or more of these modes using sand or powder to create Chladni figures on a plate with the vibrations driven by some external driver. This demonstration is a classic, but there are limitations to what can be observed. For example, Chladni patterns do not allow one to observe any aspects of the vibration except for the position of the nodes, the technique is not useful for investigating anything except horizontal flat surfaces, and it is very difficult to observe the presence of nearly nondegenerate normal modes such as those shown in Fig. 5 and discussed in Ref. 2. All of these problems are alleviated using electronic speckle pattern interferometry instead of Chladni patterns to observe the vibrations of an object.

In addition to viewing harmonic vibrations, the electronic speckle pattern interferometer is very useful for viewing changes in the index of refraction. Thus, the effects of the heat flow from a student's hand on the atmosphere is easily imaged as well as gas and fluid flow. Naturally, imaging of changes in the index of refraction can be accomplished quite inexpensively with an interferometer such as a Twyman–Green; however, the advantage of the electronic speckle pattern interferometer is that the beam can be expanded so that the area of observation is quite large, yet the size of the optics remains quite small. For example, in the electronic speckle pattern interferometer described here, the largest optical component is the 2 in. square beamsplitter. The rest of the optics is no larger than 1 in. in diameter, yet the area of observation is approximately 50 cm in diameter. To view an object of this size with a Twyman–Green interferometer would require the beamsplitters, mirrors, and lenses to be as large as the field of view and thus be extremely expensive.

IV. DISCUSSION

We note that there are several variations on the electronic speckle pattern interferometer in the literature.[10–13] These variations typically allow the user to gain phase information about the movement of the object and extend the range of the interferometer. We see no reason why many of these variations cannot be implemented with the electronic speckle pattern interferometer described here if the added information justifies the cost of implementation. Additionally, the issues discussed concerning vibration isolation and speckle size can be addressed in various ways. However, as a demonstration apparatus and for many research applications, these refinements are not necessary.

The electronic speckle pattern interferometer is especially useful when discussing normal modes of vibration. It also is very useful for viewing and measuring submicron displacements and changes in index of refraction when a large field of view is required. Unlike similar demonstrations using Chladni patterns, the object under study need not be flat or horizontal. However, the interferometer's most valuable educational use is in the advanced undergraduate laboratory. Advanced undergraduate students can investigate such phenomena as the vibrations of musical instruments, heat conduction, and fluid flow. An excellent subject for an experiment in an advanced undergraduate laboratory is the phenomenon of the splitting of normal mode doublets in a vibrating plate as discussed in Ref. 2. By using an electronic speckle pattern interferometer students can measure the resonant frequencies of a plate and show that the splitting is linearly proportional to the magnitude of the perturbing mass.

In addition to its potential for educational use, this interferometer is a useful research tool. The electronic speckle pattern interferometer has been used by many researchers for several different types of investigations.[14–18] Most of these measurements are possible with the interferometer design presented here. We hope that the simplicity and cost effectiveness of this interferometer will encourage a wider use of the technique in the classroom and in the undergraduate laboratory.

ACKNOWLEDGMENTS

This work was made possible by a generous grant from the John R. and Ruth W. Gurtler Foundation.

[a]Electronic mail: tmoore@rollins.edu

[1]R. Jones and C. Wykes, *Holographic and Speckle Interferometry*, 2nd ed. (Cambridge U.P., Cambridge, 1987).

[2]B. M. Deutsch, A. R. Robinson, R. J. Felce, and T. R. Moore, ''Nondegenerate normal-mode doublets in vibrating flat circular plates,'' Am. J. Phys. **72**, 220–224 (2004).

[3]K. Høgmoen and H. M. Pederson, ''Measurement of small vibrations using electronic speckle pattern interferometry: Theory,'' J. Opt. Soc. Am. **67**, 1578–1583 (1977).

[4]A. E. Ennos, ''Speckle interferometry,'' in *Laser Speckle and Related Phenomena*, edited by J. C. Dainty (Springer, New York, 1984), pp. 203–253.

[5]S. Nakadate, T. Yatagai, and H. Saito, ''Electronic speckle pattern interferometry using digital image processing techniques,'' Appl. Opt. **19**, 1879–1883 (1980).

[6]E. Vikhagen, ''Vibration measurement using phase shifting TV-holography and digital image processing,'' Opt. Commun. **69**, 252–256 (1989).

[7]G. Å. Slettemoen, ''Electronic speckle pattern interferometric system based on speckle reference beam,'' Appl. Opt. **19**, 616–623 (1980).

[8]O. J. Løkberg, ''ESPI: The ultimate holographic tool for vibration analysis?,'' J. Acoust. Soc. Am. **75**, 1783–1791 (1984).

[9]D. Findeis, D. R. Rowland, and J. Gryzagoridis, ''Vibration isolation techniques suitable for portable electronic speckle pattern interferometry,'' Proc. SPIE **4704**, 159–167 (2002).

[10]M. Servin, A. Davila, and J. A. Quiroga, ''Extended-range temporal electronic speckle pattern interferometry,'' Appl. Opt. **41**, 4541–4547 (2002).

[11]G. H. Kaufmann and G. E. Galizzi, ''Phase measurement in temporal speckle pattern interferometry: Comparison between the phase-shifting and the Fourier transform methods,'' Appl. Opt. **41**, 7254–7263 (2002).

[12]S. Nakadate and H. Saito, ''Fringe scanning speckle-pattern interferometry,'' Appl. Opt. **24**, 2172–2180 (1985).

[13]S. Nakadate, ''Vibration measurement using phase-shifting speckle-pattern interferometry,'' Appl. Opt. **25**, 4162–4167 (1986).

[14]D. Coburn and J. Slevin, ''Digital correlation system for nondestructive testing of thermally stressed ceramics,'' Appl. Opt. **34**, 5977–5986 (1995).

[15]O. J. Løkberg, ''Sound in flight: Measurement of sound fields by use of TV holography,'' Appl. Opt. **33**, 2574–2584 (1994).

[16]K. D. Kihm, ''Applications of laser speckle photography for thermal flow problems,'' Opt. Lasers Eng. **29**, 171–200 (1998).

[17]O. J. Løkberg, J. T. Malmo, and G. Å. Slettemoen, ''Interferometric measurements of high temperature objects by electronic speckle pattern interferometry,'' Appl. Opt. **24**, 3167–3172 (1985).

[18]T. R. Moore, J. D. Kaplon, G. D. McDowall, and K. A. Martin, ''Vibrational modes of trumpet bells,'' J. Sound Vib. **254**, 777–786 (2002).

[1]R. K. Adair, ''Comment on 'How to hit home runs: Optimum baseball swing parameters for maximum range trajectories,' '' Am. J. Phys. **73**, 184–185 (2005).
[2]R. K. Adair, *The Physics of Baseball* (HarperCollins, New York, 2002), 3rd ed.
[3]G. S. Sawicki, M. Hubbard, and W. J. Stronge, ''How to hit home runs: Optimum baseball swing parameters for maximum range trajectories,'' Am. J. Phys. **71** (11), 1152–1162 (2003).
[4]G. K. Batchelor, *An Introduction to Fluid Dynamics* (Cambridge University Press, Cambridge, UK, 1977).
[5]L. D. Landau and E. M. Lifshitz, *Fluid Mechanics* (Pergamon Press, Oxford, 1959).
[6]R. L. Street, G. Z. Watters, and J. K. Vennard, *Elementary Fluid Mechanics* (John Wiley and Sons, New York, 1996), 7th ed.
[7]R. G. Watts and R. Ferrer, ''The lateral force on a spinning sphere: aerodynamics of a curve ball,'' Am. J. Phys. **55** (1), 40–44 (1987).
[8]L. W. Alaways, S. P. Mish, and M. Hubbard, ''Identification of release conditions and aerodynamic forces in pitched-baseball trajectories,'' J. Appl. Biomechanics **17**(1), 63–76 (2001).
[9]L. W. Alaways and M. Hubbard, ''Experimental determination of baseball spin and lift,'' J. Sports Sci. **19**, 349–358 (2001).
[10]K. Aoki, Y. Kinoshita, and E. Hirota, ''The surface structure and aerodynamics of baseballs,'' in *The Engineering of Sport 4*, edited by S. Ujihashi and S. J. Haake (Blackwell Science, Oxford, UK, 2002), pp. 283–289.
[11]L. J. Briggs, ''Effect of spin and speed on the lateral deflection (curve) of a baseball; and the Magnus effect for smooth spheres,'' Am. J. Phys. **27**, 589–596 (1959).
[12]A. J. Smits and D. R. Smith, ''A new aerodynamic model of a golf ball in flight,'' in *Science and Golf II*, Proc. 1994 World Scientific Congress of Golf, edited by A. J. Cochran and M. R. Farrally (E&FN Spon, London, 1994), pp. 340–347.
[13]R. D. Mehta and J. M. Pallis, ''Sports ball aerodynamics: Effects of velocity, spin and surface roughness,'' in *Materials and Science in Sports*,edited by F. H. Froes and S. J. Haake (TMS, Warrendale, PA, 2001), pp. 185–197.
[14]E. Achenbach, ''The effects of surface roughness and tunnel blockage on the flow past spheres,'' J. Fluid Mech. **65** (1), 113–125 (1974).
[15]C. Frohlich, ''Aerodynamic drag crisis and its possible effect on the flight of baseballs,'' Am. J. Phys. **52** (4), 325–334 (1984).
[16]S. C. R. Dennis, S. N. Singh, and D. B. Ingham, ''The steady flow due to a rotating sphere at low and moderate Reynolds numbers,'' J. Fluid Mech. **101**, 267–279 (1980).
[17]R. G. Watts and S. Baroni, ''Baseball-bat collisions and the resulting trajectories of spinning balls,'' Am. J. Phys. **57**(1), 40–45 (1989).
[18]G. Tavares, K. Shannon, and T. Melvin, ''Golf ball spin decay model based on radar measurements,'' in *Science & Golf III*, Proc. 1998 World Scientific Congress of Golf, edited by M. Farrally and A. J. Cochran (Human Kinetics, Champaign, IL, 1999), pp. 464–472.
[19]The friction cone is a cone of half angle $\theta = \tan^{-1}\mu$ around the normal at the contact point, within which the contact force vector must lie if there is no slip because the tangent (frictional) component must be less than μ times the normal component.
[20]W. E. Red and A. J. Zogaib, ''Javelin dynamics including body interaction,'' J. Appl. Mech. **44**, 496–498 (1977).
[21]Baseball Almanac ⟨http://baseball-almanac.com/feats/feats1.shtml⟩.

Erratum: "A simple design for an electronic speckle pattern interferometer" [Am. J. Phys. 72 (11), 1380–1384 (2004)]

Thomas R. Moore
Department of Physics, Rollins College, 1000 Holt Avenue, Winter Park, Florida 23789

(Received 12 October 2004; accepted 15 October 2004)

[DOI: 10.1119/1.1830506]

Figure 5 of this manuscript was printed incorrectly. The correct figure is shown below.

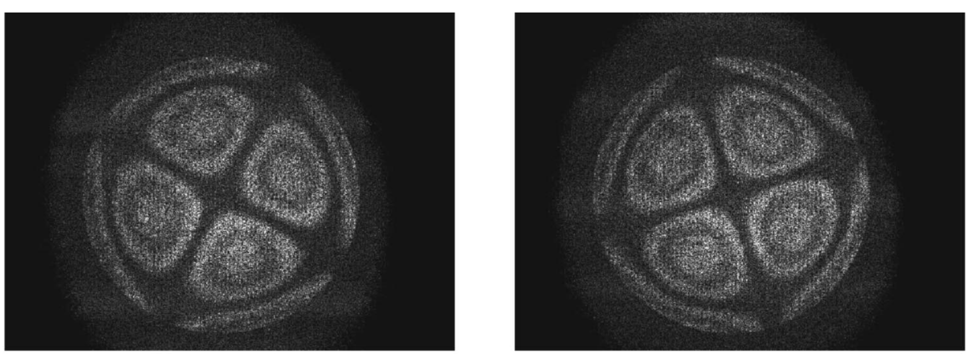

Fig. 5. Interferograms of a 17 cm circular plate vibrating in one of its normal modes. Theoretically the two modes occur at the same frequency, however, the degeneracy is broken by a slight asymmetry in the plate. The frequencies of vibration are 2133 and 2145 Hz.

